Hindawi
Advances in Civil Engineering
Volume 2018, Article ID 5159218, 10 pages
https://doi.org/10.1155/2018/5159218

Research Article

Scheme Exploration and Performance Analysis of 800-Meter Superlarge Span Structure

Deshen Chen,[1] Hongliang Qian,[1] Huajie Wang,[1] and Yue Wu[2]

[1]*Department of Civil Engineering, Harbin Institute of Technology at Weihai, Weihai 264209, China*
[2]*School of Civil Engineering, Key Laboratory of Structures Dynamic Behavior and Control of the Ministry of Education, Harbin Institute of Technology, Harbin 150090, China*

Correspondence should be addressed to Hongliang Qian; qianhl@hit.edu.cn

Received 11 June 2018; Accepted 1 August 2018; Published 3 September 2018

Academic Editor: Rosario Montuori

Superlarge span structure is one of the important trends for future building development. Under the background of the 800-meter superlarge span dome project proposed by China Construction Group, this paper focuses on the structural optimization and performance analysis of this superlarge span structure. The previous ideas of the superdome and the maximum span of existed spatial structures are reviewed, and some structural form selection principles are put forward which lay foundation for structural selection. The applicability of high-strength steel and aluminum alloy is also discussed. It is demonstrated that the high-strength steel and aluminum alloy contribute little to structural comprehensive performances. Then, considering the effects of grid division, members topological relation, and surface shape, six kinds of rigid systems are contrastively studied to determine the optimal scheme. The structural performances along with the increasing span are explored in detail. To further reduce the structural weight and improve mechanical performance, a new composite scheme and the cable-stayed megastructure are proposed and studied. The research methods and performance analysis results can provide significant references for the following research on the superlarge span structure.

1. Introduction

As new materials and advanced engineering technologies increasingly emerge, the development of the large span spatial structure has made great strides and the concept of the superlong span dome has been put forward. Such a superdome can keep a warm and humid climate inside even when built in the cold and dry area. Moreover, by unified planning in such a grander scale, the superdome can also make a significant contribution to energy saving and emission reduction of the modern cities.

From the 1960s, some leading architects began to dig into this field and raised a number of conceptual designs. Fuller put forward a famous project named "Manhattan dome" [1]. A super geodesic dome in the size of 3200 m diameter and 1600 m height is designed to cover the Manhattan block. It not only provides a comfortable environment but also reduces the large expenses of air conditioning and winter snow removal. Frei Otto proposed a superdome project named "the Arctic city" [2], a 2000 m diameter inflatable membrane dome built in the Arctic, and aimed at improving the working condition for polar scientists, as shown in Figure 1(a). Besides, to resist hurricanes and heat waves, American engineers proposed to build a superdome in the size of 1600 m diameter and 450 m height over Houston [3], as shown in Figure 1(b). The design consulted the three-layer structure of the Garden of Eden in Britain. An American company specializing in the design and installation of the cable membrane structure proposed the "Spantheon system" for the superlong span dome, as shown in Figure 1(c). It consists of a number of huge arch trusses covered by the light cable membrane structure [4]. But this research field has just started in China. China Construction Group is carrying out the project named "TianQiong," as shown in Figure 1(d). The project is an 800-meter span superdome isolating the external harsh natural condition and simulating the real climate inside. The tropical ocean even lifestyle can be created in severe cold regions.

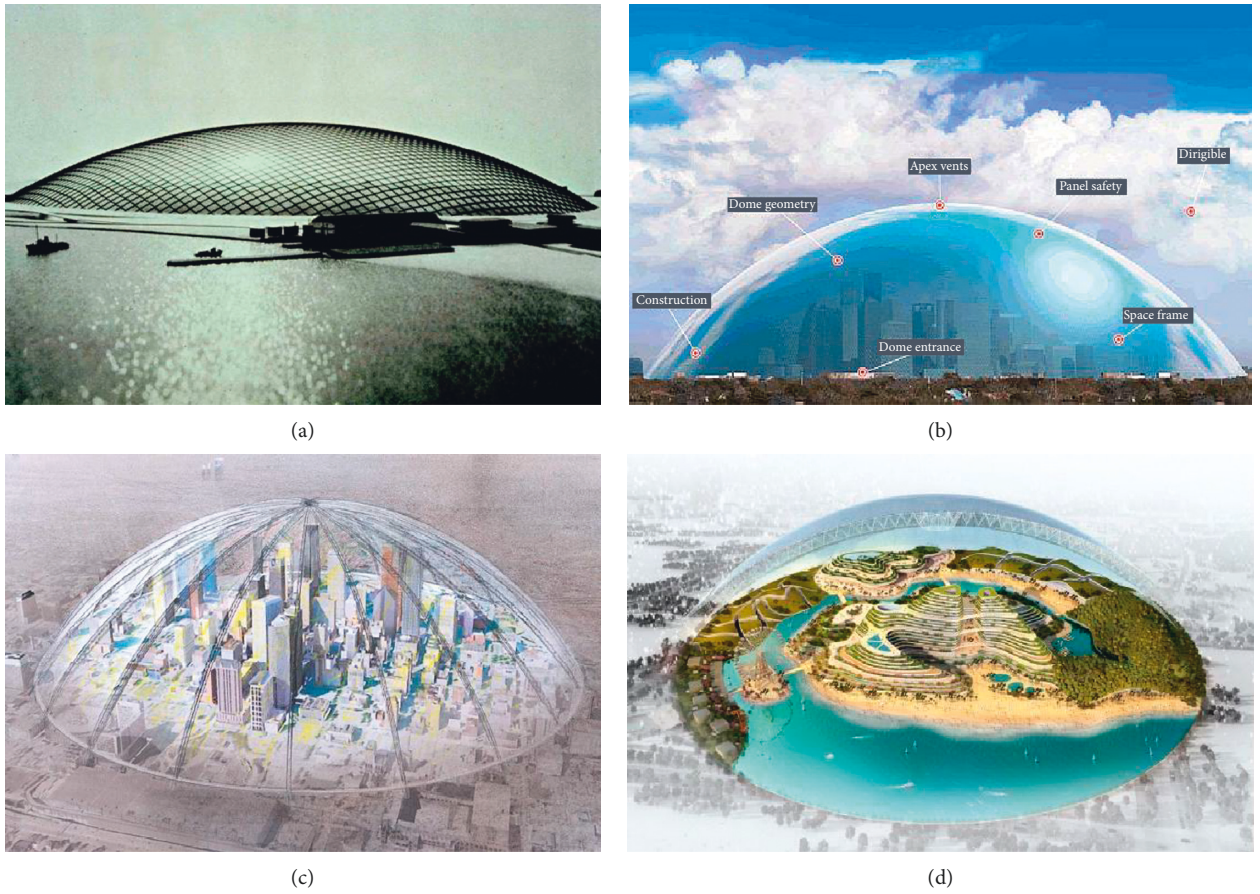

Figure 1: Some superlong span dome projects: (a) the Arctic city; (b) Houston dome; (c) Spantheon structure; (d) Tian Qiong.

This paper initially explores the comprehensive performance of the 800-meter span structure. Some basic principles are put forward, and the applicability of high-strength steel and aluminum alloy is also discussed. Six rigid structural systems and two rigid-flexible composite schemes are studied by the numerical method. The changes of structural performance along with the increasing spans are also given. Then, the optimum scheme for the 800 m span superdome, in certain conditions, will be obtained through contrastive analysis.

2. Design Principle and Material Selection

2.1. Representative Works of Spatial Structures. Table 1 gives representative projects of the common spatial structure forms which have the largest spans. It can be seen clearly that the maximum span of the spatial structure has already exceeded 300 m, and the suspension bridge has reached nearly 2000 m. What kind of structural system is the best choice for the superdome? From the existing engineering practices, some basic principles can be summed up: (1) the transmission path of internal force should be simple and efficient. The components mainly in axial stress can make full use of material properties. (2) The light roofing material should be used to cover the larger area with less material and improve the daylighting. (3) The main structure should be landed on the ground, and the horizontal thrust needs to be reduced as far as possible to relieve the pressure of foundation.

2.2. Load Values and Design Combinations. The loads in the design stage consider dead load, live load, wind load, and temperature effect. The dead load includes the roof load and the weight of structural components. The roof load is calculated by the developed area in the value of 100 kg/m^2. The live load is calculated by the projection area in the value of 50 kg/m^2. According to the Chinese load code for the design of building structures (GB50009-2012) [19], the wind load takes the B class of surface roughness. The basic wind pressure is 0.5 kN/m^2, and the wind vibration coefficient is 1.6. The shape coefficient is taken according to the rotating dome in Table 8.3.1 of the Chinese load code (GB50009-2012). The whole structure temperature effect is considered as $\pm 30^{\circ}$C. The load combinations of the bearing capacity limit state are shown in Table 2. When it comes to structural serviceability limit state, load combinations only consider the combined factor in Table 2.

2.3. Structural Control Indexes. Strength index is the stress ratio of member cross section in the full stress design, and the limit is 0.8 with the consideration of member stability.

Table 1: Representative works of different spatial structure forms.

Forms	Representative works	Span (m)	Country	Time	Characteristics
Flatbed grid	Indoor football field of Shenyang Expo Center [5]	144	China	2001	Two-way orthogonal positive grid
	Wuhan Optics Valley Tennis Center [6]	151	China	2015	Three-layer grid with middle retractable roof
Reticulated shell	Fukuoka Dome [7]	222	Japan	1993	Retractable roof composed of three fan-shaped shells
	Shenyang Culture and Art Center [8]	110	China	2013	Single-layer folded plate shell
Megastructure	Gymnasium of Dalian Sports Center [9]	145	China	2013	Ellipse-shaped megastructure suspendome
Pipe truss arch	Dongsheng Stadium in Ordos [10]	330	China	2011	Quadrilateral tube truss arch
	Gabon National Stadium [11]	320	Gabon	2011	Inverted triangle truss arch
String structure	Dongying Yellow River Estuary Model Hall [12]	148	China	2009	Unidirectional truss string structure
	Jinan Olympic Sports Center Stadium [13]	122	China	2008	Suspended lattice shell
Cable structure	Millennium Dome [14]	320	Britain	1998	Cable net with 12 mast supports
	The Centennial Olympics Stadium [15]	191	America	1996	Ellipse plane cable dome
	The Akashi Kaikyo Bridge (Kitagawa 2004)	1991	Japan	1999	Suspension bridge
Membrane structure	Shanghai World Expo Axis [16]	110	China	2009	Tensile membrane structure
	Baseball Hall of Tokyo [17]	205	Japan	1988	Gas-bearing membrane structure
	Vista Alegre [18]	50	Spain	2001	Moored floating structure

For the cables, the maximum axial force in the ultimate state of load capacity is not more than 0.5 times the minimum breaking force and cables in the main structure are not allowed to appear slack. In addition, according to the technical specification for space frame structures (JGJ7-2010) [20], the deflection limit of single-layer and double-layer latticed shells are L/400 and L/250, respectively, and L is the structural span. In this study, the deflection limit is assumed to L/500. With the span increasing, the stability has gradually become the control factor of the design. The elastic-plastic stability coefficient is calculated under the standard combination of the dead load and live load, and the elastic stability coefficient is also used as a reference.

2.4. Material Selection. Taken the double-layer reticulated shell in the span of 800 m and height of 200 m for instance, the applicability of high-strength steel and aluminum alloy is discussed. According to the code for the design of steel structures (GB50017-2003) [21], the code for the design of high-strength steel structures (under preparation) [22, 23] and the code for the design of aluminum structures (GB50429-2007) [24], three types of high-strength steel including Q420, Q690, and Q960 and the high-strength aluminum alloy 6061 T6 are selected for the structural design. The Q420 type is designed according to the front two codes, respectively (Q420S for the steel structures code and Q420 for the high-strength steel structures code).

The material consumption, deflection, and stability performance are shown in Figure 2. Compared with Q420S, 6061 T6 type can almost reduce structural weight by half, but the deflection increases about 65.8%. The density and elastic modulus of the aluminum alloy is only about 1/3 of steel. The member section and material volume usage are both larger, and the structure stability becomes worse. Besides, the welding performance of the aluminum alloy is poor, and joint connection is more difficult. The material consumption of Q420 can be reduced by 7.7% compared with Q420S.

Table 2: Load combinations of the bearing capacity limit state (partial factor × combined factor).

No.	Combination	Dead load	Live load	Wind load	Temperature
1	D + L	1.35 × 1.0	1.4 × 0.7	—	—
2	D + L	1.2 × 1.0	1.4 × 1.0	—	—
3	D + L + T	1.35 × 1.0	1.4 × 0.7	—	1.4 × 0.6
4	D + L + T	1.2 × 1.0	1.4 × 1.0	—	1.4 × 0.6
5	D + L + W	1.35 × 1.0	1.4 × 0.7	1.4 × 0.6	—
6	D + L + W	1.2 × 1.0	1.4 × 1.0	1.4 × 0.6	—
7	D + L + W	1.2 × 1.0	1.4 × 0.7	1.4 × 1.0	—
8	D + L + W + T	1.35 × 1.0	1.4 × 0.7	1.4 × 0.6	1.4 × 0.6
9	D + L + W + T	1.2 × 1.0	1.4 × 1.0	1.4 × 0.6	1.4 × 0.6
10	D + L + W + T	1.2 × 1.0	1.4 × 0.7	1.4 × 1.0	1.4 × 0.6
11	D + W	1.0 × 1.0	—	1.4 × 1.0	—
12	D + W + T	1.0 × 1.0	—	1.4 × 1.0	1.4 × 0.6

From Q420 to Q960, the material consumption only decreases by 7.0% which indicates that raising material strength contributes little to the economy. The deflection is almost inversely proportional to the material consumption. The elastic stability coefficients decrease while the elastic-plastic stability coefficients increase. Because the elastic stability coefficient is mainly affected by the member section, and the elastic-plastic stability coefficient is mainly affected by the yield point of the material. Therefore, the application of high-strength steel and aluminum alloy has little improvement in the structural comprehensive performances. Therefore, the Q420S type is used in the following scheme study. Besides, the cable in strength of 1860 MPa is used according to the technical specification of cable structures (JGJ257-2012) [25].

3. Rigid Structural Systems for the Superdome

Rigid structural systems are the most widely used forms in spatial structures. The reticulated shell and reticulated

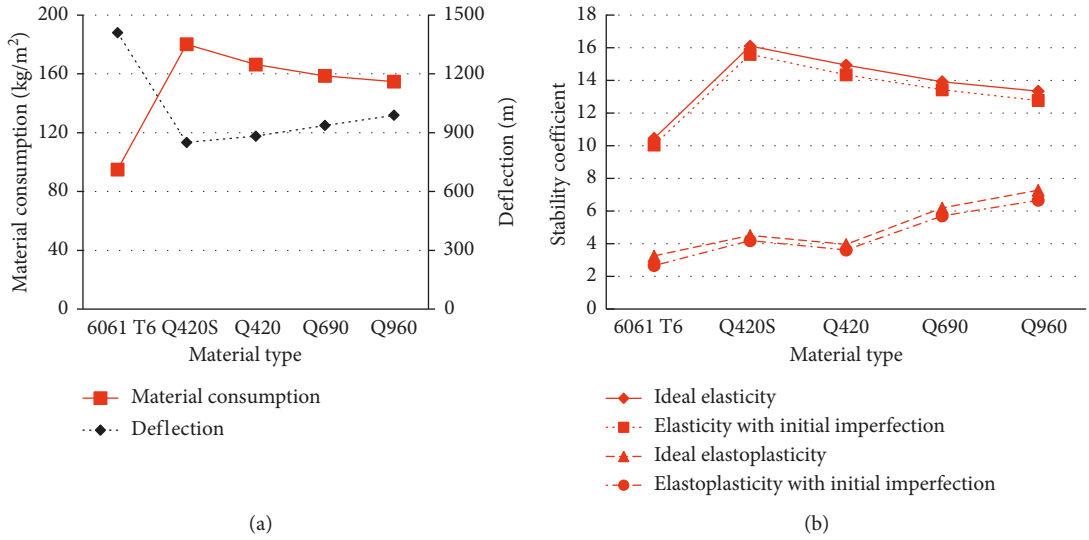

Figure 2: Comparison of different material types: (a) material consumption and deflection; (b) stability coefficient.

megastructure are all typical representatives. They have the concise and efficient load transfer path, and the structures are mainly in the state of membrane stress while the components are axially loaded.

3.1. Structural Design. The reticulated shell and reticulated megastructure are studied considering the effects of grid division, members topological relation, and surface shape. As shown in Figure 3, six forms are involved in this study including Kiewitt pyramidal spherical reticulated shell (KPS), geodesic pyramidal spherical reticulated shell (GPS), Kiewitt pyramidal catenoid reticulated shell (KPC), Kiewitt spherical reticulated megastructure (KSM), rib-circle spherical reticulated megastructure (RSM), and rib-circle-reinforced spherical reticulated megastructure (RRSM). The structural span is 800 m, and the height is 200 m. According to the technical specification for space frame structures (JGJ7-2010), the ratio of thickness to span is between 1/60 and 1/30, and the practical ratio decreases gradually with the increase of span. In this study, the ratio of thickness to span is 1/80. For the reticulated megastructure, the size and height of space truss are both 20 m while in the strengthened region, these values are both 10 m. Structures are all supported by fixed hinge bearings of bottom chords and radial constraints are all released. Seen from the top view, the megastructure has better daylighting performance than the reticulated shell.

Figure 4 gives the statistical graphs for member section distribution of different schemes. For the reticulated shells, more than 98% of components have sections smaller than $\phi 800 \times 24$ mm, and the biggest section is 2400×76 mm. For the reticulated megastructures, about 70% of components have section smaller than $\phi 800 \times 24$ and the biggest section is 3600×120 mm. The element amount of RRSM is obviously more than the other two schemes. More than 83% of components have sections smaller than $\phi 800 \times 24$ mm. For the member section design, more than 85% of members are controlled by the design load combination of the dead load and live load. The wind load and temperature effect have little effect on the design internal force.

3.2. Performance Analysis. Figure 5 shows the analysis results of steel consumption, deflection, and stability performance. For the reticulated shells, the steel consumption of the geodesic type is 2.3% lower than the Kiewitt type, but the deflection is 12.3% larger than the latter. The catenoid reticulated shell consumes 3.9% more steel and has 5.6% smaller deflection than the spherical reticulated shell. There is little difference of stability performance among three schemes. For the reticulated megastructures, the steel consumption of the Kiewitt type is 3.1% higher than the rib-circle type, but the deflection is 5.9% smaller than the latter. The rib-circle-reinforced type consumes 12.3% more steel and has 6.0% smaller deflection than the rib-circle type. Moreover, the rib-circle type has the poorer stability performance than the other two schemes. On the whole, the reticulated shells have relatively smaller material consumption and deflection than the reticulated megastructures. The stability performance is similar and little subjected to the influence of imperfection. Considering the structural design and overall structural performance, the Kiewitt pyramidal spherical reticulated shell and Kiewitt spherical reticulated megastructure are the optimal schemes.

For these two schemes, considering the structural span range from 100 m to 800 m with the increment of 100 m, the structural performances along with increasing spans are explored. Figure 6 shows the analysis results for steel consumption, deflection, and stability performance. The steel consumption and deflection of these two schemes both increase as the structural span becomes larger. The megastructure always consumes a little more steel material than the reticulated shell, and the former has larger deflection than the latter. As the structural span increases, the differences of steel consumption are almost invariants all

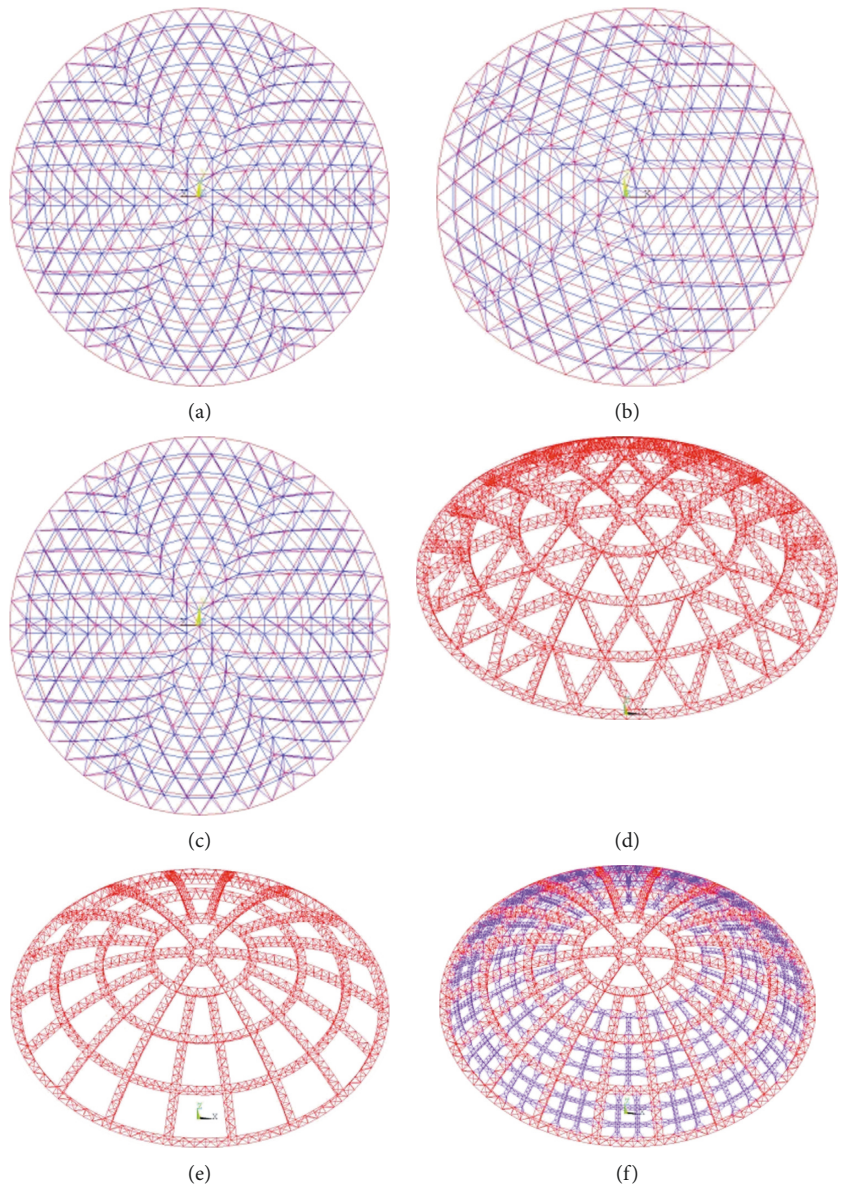

Figure 3: Six kinds of traditional rigid structural systems: (a) Kiewitt triangular pyramidal spherical reticulated shell (KPS); (b) geodesic triangular pyramidal spherical reticulated shell (GPS); (c) Kiewitt triangular pyramidal catenoid reticulated shell (KPC); (d) Kiewitt spherical reticulated megastructure (KSM); (e) rib-circle spherical reticulated megastructure (RSM); (f) rib-circle-reinforced spherical reticulated megastructure (RRSM).

around 20 kg/m^2, while the differences of the deflection become larger changing from 25 to 125 mm. Besides, for the stability performance, the elastoplastic stability coefficient of the reticulated shell considering initial imperfection goes down faster than the megastructure. When the span is larger than 300 m, the megastructure has better stability performance.

4. Rigid-Flexible Composite Systems for the Superdome

From the rigid system above, the great structural weight is the most important load and even becomes a key factor for determining the feasibility of the scheme. To improve the structural performance and reduce the structural weight, the rigid-flexible composite systems consisting of rigid components and flexible cables are taken into consideration. Because of the enormous support reaction the shell has to be supported on the ground. In order to obtain enough service space, the combination of the central suspended lattice shell and double-reticulated shell around can be a new scheme. This new composite scheme and the cable-stayed megastructure are taken into consideration for the superdome.

4.1. Structural Design. The rigid-flexible composite schemes are shown in Figures 7(a) and 7(b). For the new composite scheme, the rigid substructure is the K6 pyramid spherical reticulated shell in the grid division of 40 loops. The thickness

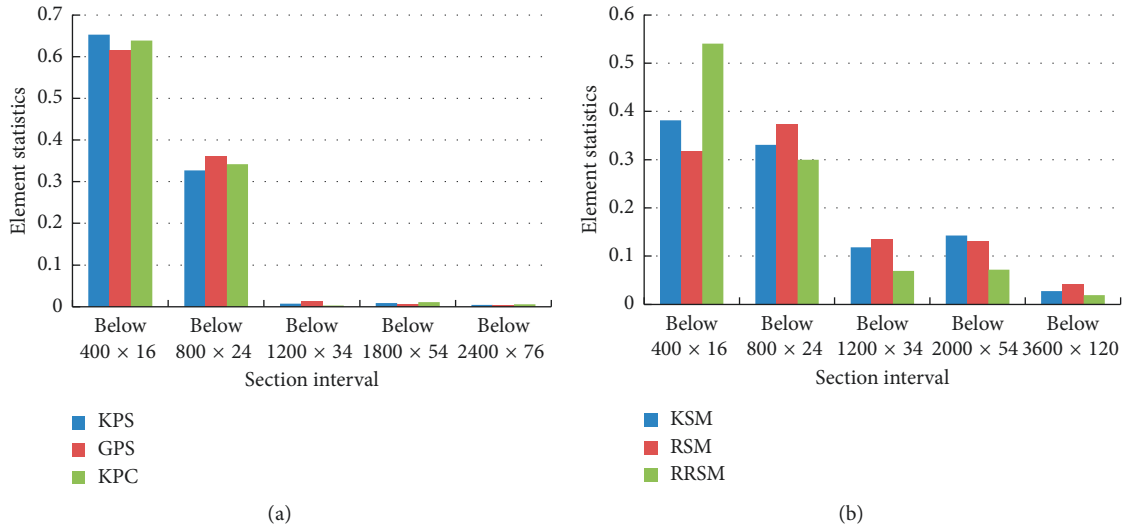

Figure 4: Member section statistics of six schemes: (a) reticulated shells; (b) reticulated megastructure.

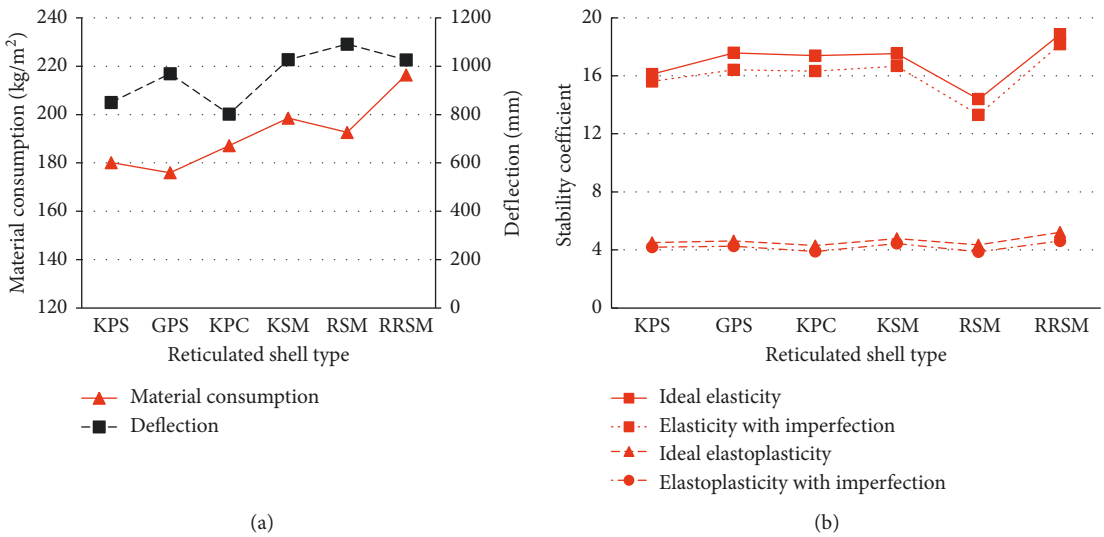

Figure 5: Structural performances of different schemes: (a) material consumption and deflection; (b) stability coefficient.

is 10 m, and the top 17 loops are replaced by the suspended lattice shell. There are 16 groups of hoop cables in the horizontal distance of 12 m. From inside out, every group of hoop cables has a corresponding number from 1 to 16. The cable-stayed megastructure is composed of rib-circle spherical reticulated megastructure and 9 groups of stay cables. The main ribs are made up of three-layer space truss, and each group of stay cables has four cables connected with adjacent nodes of intersection on main ribs. The structural spans are both 800 m, and the height is 200 m; they are both supported by fixed hinge bearings, and radial constraints are all released.

The design process of rigid-flexible composite systems is shown in Figure 8. Fully stressed design and form-finding analysis should be carried out repeatedly and alternately until the structure gets to a steady state. The inverse iteration method is used to adjust the structural lofting state shape, and the tension compensation method is used to adjust the cable initial pretension of the lofting state [26]. The control indexes of form-finding analysis are geometric configuration deviation and cable pretension design value deviation in the prestressed equilibrium state.

4.2. Performance Analysis. Figure 9 gives the pretension design results and the ratio of pretension to breaking force for each hoop cable of the new composite scheme. The cable pretension increases from the inside out. The cables in external loops contribute more to the structure. The pretension design values of the cable-stayed megastructure are 7622 kN of inner stay cables and 10857 kN of outer stay cables.

The element ratio statistics of rigid components are shown in Figure 10. The steel usage of the new composite scheme is 170.1 kg/m^2, which is 5.6% less than the double-layer reticulated shell scheme. In the part of the double-layer

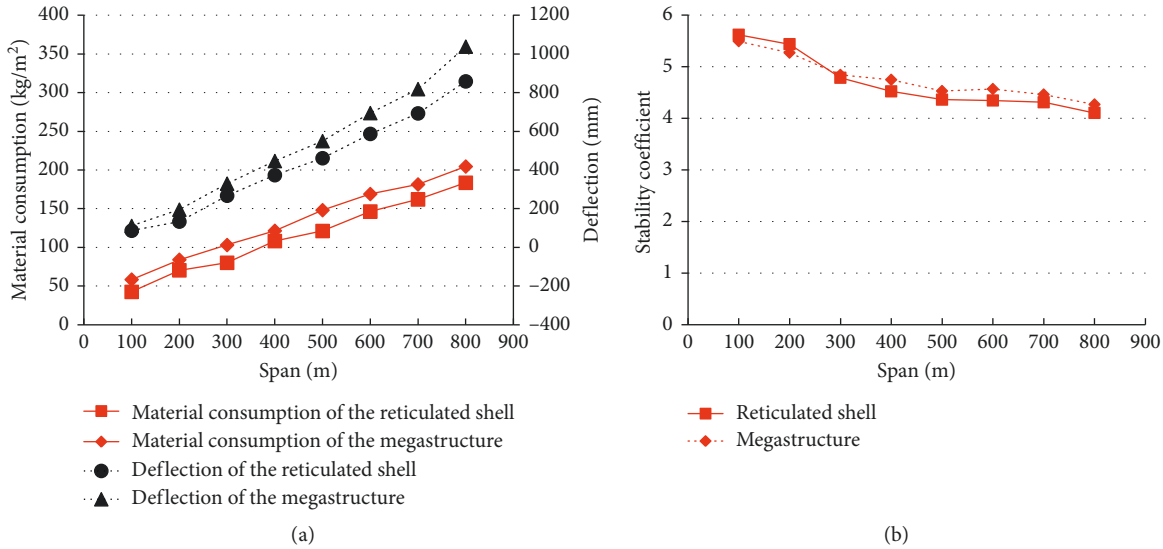

Figure 6: Relation of structural performances and increasing spans: (a) material consumption and deflection; (b) stability coefficient.

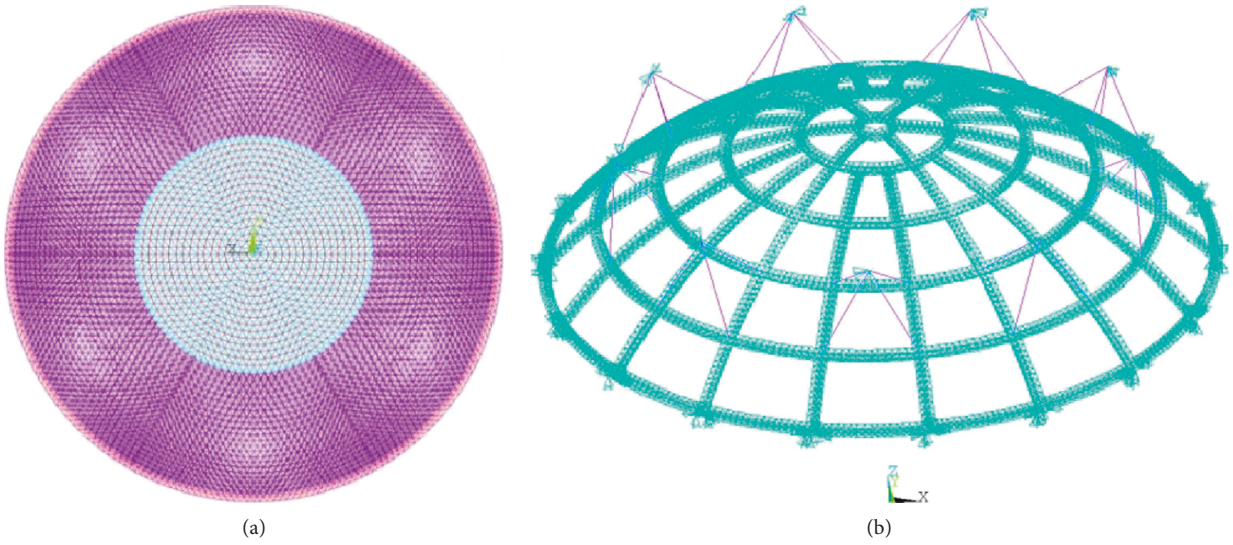

Figure 7: Rigid-flexible composite schemes: (a) new composite scheme; (b) the cable-stayed megastructure.

reticulated shell, more than 90% of components have sections smaller than $\phi 600 \times 20$ mm. However, the central suspended lattice shell obviously has much bigger sections. More than 94% of components have sections greater than $\phi 600 \times 20$ mm, and the biggest section is 2800×58 mm. For the cable-stayed megastructure, the steel consumption is 140.5 kg/m^2, which is 29.2% less than the megastructure scheme. More than 71% of components have sections smaller than $\phi 400 \times 16$ mm, and the biggest section is 1600×38 mm.

Figure 11 shows the displacement under the load case of the dead and live loads under the limit state of serviceability. The component weight is taken into consideration when solving the structural stretch-forming state, and the maximum deformations of the new composite scheme and cable-stayed megastructure are 0.55 m and 1.19 m. Besides, the elastic-plastic stability coefficients of the new composite scheme and cable-stayed megastructure can reach 3.42 and 4.59. When L/300 initial imperfection is considered, these coefficients are 2.94 and 4.37, respectively. Therefore, the cable-stayed megastructure has lower steel consumption and good daylighting performance. The section size of steel members has also been reduced effectively. But the height of the host tower, which is ignored in simulation, is over 200 m, and the difficulty of construction increases overall.

5. Conclusions

This paper initially explores the suitable structural systems including rigid systems and rigid-flexible composite systems for the 800 m span superdome. Some conclusions can be drawn as follows:

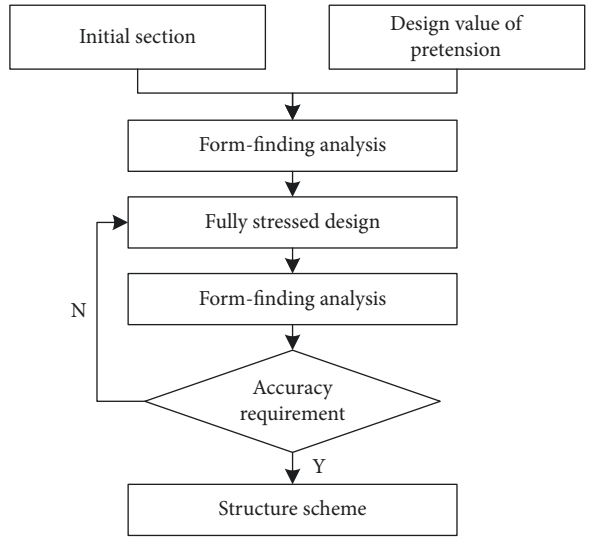

Figure 8: Design process of the rigid-flexible composite scheme.

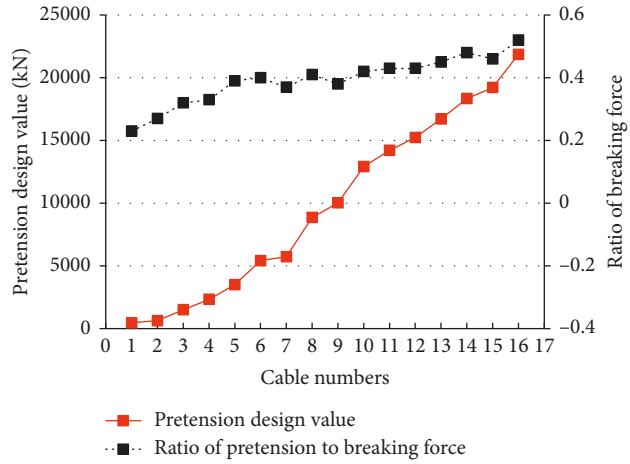

Figure 9: Design results of ring cables.

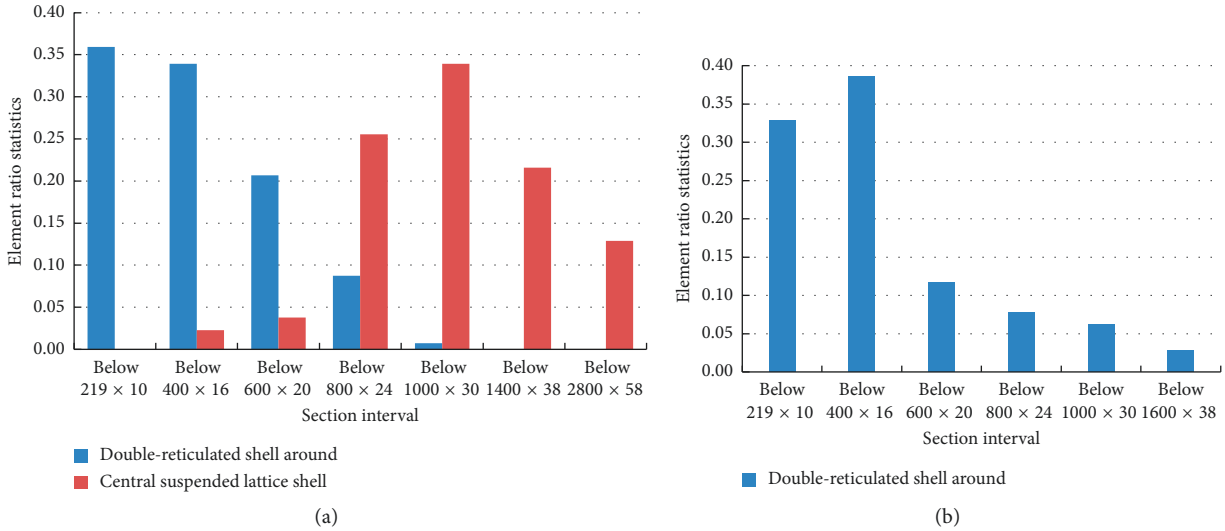

Figure 10: Element ratio statistics of rigid components: (a) new composite scheme; (b) cable-stayed megastructure.

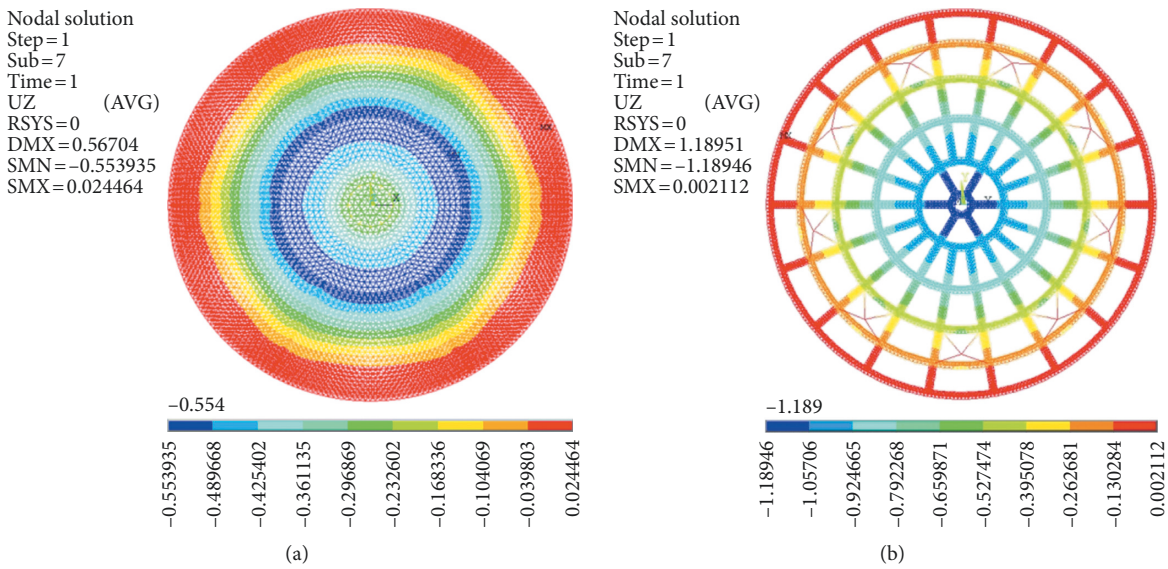

Figure 11: Displacement under the load case of the dead and live loads: (a) new composite scheme; (b) cable-stayed megastructure.

(1) The application of the high-strength steel and aluminum alloy has little improvements in structural performances. High-strength improves the elastic-plastic stability but contributes little to the material consumption. Aluminum alloy significantly reduces the structural weight, but the member section and material volume usage both increase and the structure stability becomes worse.

(2) Considering the effects of grid division, members topological relation, and surface shape, the Kiewitt pyramidal spherical reticulated shell and Kiewitt spherical reticulated megastructure are the optimal rigid systems. The steel consumptions are 180.1 kg/m^2 and 198.5 kg/m^2, respectively.

(3) As the structural span becomes larger, the steel consumption and deflection both increase and the megastructure always consumes a little more material and has larger deflection than the reticulated shell. When the span is larger than 300 m, the megastructure has better stability performance.

(4) A new composite scheme and the cable-stayed megastructure are proposed for the superdome. The cable-stayed megastructure has lower steel consumption with the value of 140.5 kg/m^2 and better structure stability. The section size of steel members has also been reduced effectively.

Data Availability

The data used to support the findings of this study are available from the corresponding author upon request.

Conflicts of Interest

The authors declare that they have no conflicts of interest.

Acknowledgments

The authors gratefully acknowledge the support of the National Key Research and Development Program of China (no. 2016YFC0802003) and the National Natural Science Foundation of China (no. 51578186).

References

[1] P. Steadman, "Energy and patterns of land use," *Journal of Architectural Education*, vol. 30, no. 3, pp. 62–67, 1976.

[2] I. S. Pinto, "Lightweight and transparent domes," *International Journal of Architectural Research*, vol. 6, no. 3, pp. 124–134, 2012.

[3] R. Engelkemeir, S. D. Khan, and K. Burke, "Surface deformation in Houston, Texas using GPS," *Tectonophysics*, vol. 490, no. 1-2, pp. 47–54, 2010.

[4] Y.-G. Zhang, S.-D. Xue, Q.-S. Yang, and F. Fan, *Large Span Spatial Structure*, China Machine Press, Beijing, China, 2nd edition, 2014, in Chinese.

[5] J. Ni, B. Cai, and G. Zhou, "Structural design of the roof of the indoor football stadium in Shenyang Exhibition Center," *Progress in Steel Building Structures*, vol. 5, no. 3, pp. 1–5, 2003, in Chinese.

[6] L.-F. Zeng, W.-G. Dong, S.-Q. Wen, and X. Wang, "Resist progressive collapse analysis of the Optics Valley Tennis Center," in *Proceedings of the Second International Conference on Large Buildings of Steel and Composite Structures*, pp. 481–489, Shanghai, China, 2014.

[7] T. Yoshio, S. Yukio, and N. Masayoshi, "Fukuoka Dome, Japan," *Structural Engineering International*, vol. 4, no. 3, pp. 151–153, 1994.

[8] B.-B. Zhu, Y.-R. Lin, X.-M. Xu, and Q.-Y. Zhou, "Study on the key technologies of structural design of Shenyang Culture and Art Center," *Building Structures*, vol. 1, pp. 368–371, 2012, in Chinese.

[9] G.-B. Nie, F. Fan, and X.-D. Zhi, "Test on the suspended dome structure and joints of Dalian Gymnasium," *Advances in Structural Engineering*, vol. 16, no. 3, pp. 467–485, 2013.

[10] Z.-G. Mu, J. Xiao, Y.-L. Shen, and Z. Fan, "Study on the arc-cable supported long span spatial structure of Erdos Dong-Sheng Stadium," *Advanced Materials Research*, vol. 433–440, pp. 1836–1839, 2012.
[11] D.-J. Cao, C.-X. Hao, and F. Liu, "Design of the canopy structure of Gabon National Stadium," *Building Science*, vol. 3, pp. 87–89, 2011, in Chinese.
[12] J.-Z. Wu, M.-L. Liu, B. Shen, and Y.-H. Zhang, "Vibration frequency testing and theoretical model research on cable of truss string structure," *Building Structures*, vol. 42, no. 10, pp. 79–82, 2012, in Chinese.
[13] X.-J. Zhou, "Structural design and health monitoring of Jinan Olympic Sports Center," *Engineering Mechanics*, vol. 27, no. 2, pp. 105–113, 2010.
[14] I. Liddell, T. Mclaughlin, T. Ross, and J. Phillips, "Engineering design of the Millennium Dome," *Proceedings of the Institution of Civil Engineers-Civil Engineering*, vol. 138, no. 5, pp. 42–51, 2000.
[15] M. Kiuri and S. Reiter, "Olympic stadium design: past achievements and future challenges," *International Journal of Architectural Research*, vol. 7, no. 2, pp. 102–117, 2013.
[16] M. Kitagawa, "Technology of the Akashi Kaikyo bridge," *Structural Control and Health Monitoring*, vol. 11, no. 2, pp. 75–90, 2004.
[17] J. Knippers, "From model thinking to process design," *Architectural Design*, vol. 83, no. 2, pp. 74–81, 2013.
[18] F. V. Jensen, *Cover Elements for Retractable Roof Structures*, University of Cambridge, Cambridge, UK, 2001.
[19] GB50009-2012, *Load Code for the Design of Building Structures*, China Architectural & Building Press, Beijing, China, 2012.
[20] JGJ7-2010, *Technical Specification for Space Frame Structures*, China Architectural & Building Press, Beijing, China, 2010.
[21] GB50017-2003, *Code for Design of Steel Structures*, China Architectural & Building Press, Beijing, China, 2003.
[22] H. Ban, G. Shi, Y. Shi, and Y. Wang, "Overall buckling behavior of 460 MPa high strength steel columns: experimental investigation and design method," *Journal of Constructional Steel Research*, vol. 74, pp. 140–150, 2012.
[23] G. Shi, H. Ban, and F. Bijlaard, "Tests and numerical study of ultra-high strength steel columns with end restraints," *Journal of Constructional Steel Research*, vol. 70, pp. 236–247, 2012.
[24] GB50429-2007, *Code for Design of Aluminum Structures*, China Architectural & Building Press, Beijing, China, 2007.
[25] JGJ257-2012, *Technical Specification for Cable Structures*, China Architectural & Building Press, Beijing, China, 2012.
[26] X. F. Yuan and S. L. Dong, "Nonlinear analysis and optimum design of cable domes," *Engineering Structures*, vol. 24, no. 7, pp. 965–977, 2002.